

Red blood cell exposure increases chondrocyte susceptibility to oxidative stress following hemarthrosis



Andy J. Lee ^{*}, Lianna R. Gangi ^{*}, Fereshteh Zandkarimi [†], Brent R. Stockwell ^{† ‡},
Clark T. Hung ^{* §}

^{*} Department of Biomedical Engineering, Columbia University, 351 Engineering Terrace, Mail Code 8904, 1210 Amsterdam Avenue, New York, NY, USA

[†] Department of Chemistry, Columbia University, 216 Havemeyer Hall, 3000 Broadway, Mail Code 3183, New York, NY, USA

[‡] Department of Biological Sciences, Columbia University, 1208 NWC Building, 550 West 120th St. M.C. 4846, New York, NY, USA

[§] Department of Orthopaedic Surgery, Columbia University, New York, NY, USA

ARTICLE INFO

Article history:

Received 13 December 2022

Accepted 13 June 2023

Keywords:

Hemarthrosis
Hemophilic arthropathy
Iron
Erythrocyte
Ferroptosis

SUMMARY

Objective: The detrimental effects of blood exposure on articular tissues are well characterized, but the individual contributions of specific whole blood components are yet to be fully elucidated. Better understanding of mechanisms that drive cell and tissue damage in hemophilic arthropathy will inform novel therapeutic strategies. The studies here aimed to identify the specific contributions of intact and lysed red blood cells (RBCs) on cartilage and the therapeutic potential of Ferrostatin-1 in the context of lipid changes, oxidative stress, and ferroptosis.

Methods: Changes to biochemical and mechanical properties following intact RBC treatment were assessed in human chondrocyte-based tissue-engineered cartilage constructs and validated against human cartilage explants. Chondrocyte monolayers were assayed for changes to intracellular lipid profiles and the presence of oxidative and ferroptotic mechanisms.

Results: Markers of tissue breakdown were observed in cartilage constructs without parallel losses in DNA (control: 786.3 (102.2) ng/mg; RBC_{INT}: 751 (126.4) ng/mg; $P = 0.6279$), implicating nonlethal chondrocyte responses to intact RBCs. Dose-dependent loss of viability in response to intact and lysed RBCs was observed in chondrocyte monolayers, with greater toxicity observed with lysates. Intact RBCs induced changes to chondrocyte lipid profiles, upregulating highly oxidizable fatty acids (e.g., FA 18:2) and matrix disrupting ceramides. RBC lysates induced cell death via oxidative mechanisms that resemble ferroptosis.

Conclusions: Intact RBCs induce intracellular phenotypic changes to chondrocytes that increase vulnerability to tissue damage while lysed RBCs have a more direct influence on chondrocyte death by mechanisms that are representative of ferroptosis.

© 2023 Osteoarthritis Research Society International. Published by Elsevier Ltd. All rights reserved.

Introduction

Hemarthrosis, or bleeding of the joint space, can occur spontaneously such as is in the case of hemophilia patients, with the 12-month prevalence reaching one-third of children (age < 18 years) and two-thirds of adults (age ≥ 18 years) despite current treatments

as demonstrated in a 2018 retrospective database study¹. In addition, hemarthrosis can result from traumatic joint injury, such as anterior cruciate ligament (ACL) or meniscal tears and also as a postoperative comorbidity of common orthopedic procedures (e.g., osteochondral autograft transplantation and ACL reconstruction)^{2–4}. Clinical observations have estimated the relative volume of infiltrating blood to reach 100% (v/v) in the synovial fluid, as the volume of synovial fluid is negligible in comparison to infiltrating blood⁵. In support of strategies to mitigate the impacts of joint bleeding, Myers and co-workers found that 69% of dogs exhibited synovitis in the osteoarthritic knee 10 weeks after ACL transection. However, when electrocautery and irrigation to remove intra-articular blood prior to joint closure were implemented to maintain homeostasis, synovitis was present in only 24% of knees at the same timepoint. Iron

* Address correspondence and reprint requests to: Clark T. Hung, Department of Biomedical Engineering, Columbia University, 351 Engineering Terrace, Mail Code 8904, 1210 Amsterdam Avenue, New York, NY 10027. Tel: (212) 854 – 6542, Fax: (212) 854 – 8725.

E-mail addresses: jl3924@columbia.edu (A.J. Lee), lrg2147@columbia.edu (L.R. Gangi), fz2262@columbia.edu (F. Zandkarimi), bstockwell@columbia.edu (B.R. Stockwell), cth6@columbia.edu (C.T. Hung).

<https://doi.org/10.1016/j.joca.2023.06.007>

1063-4584/© 2023 Osteoarthritis Research Society International. Published by Elsevier Ltd. All rights reserved.

deposits were present in 75% of synovial samples obtained after routine ACL transection, but in only 6% when homeostasis was maintained⁶. It is speculated that together with reports showing better functional outcomes in patients who undergo immediate repair of the ACL following transection compared to those who receive delayed (6 weeks postinjury) repair, that joint bleeding effects may contribute to the development of post-traumatic osteoarthritis in not only patients who suffer from ACL transection, but also other common orthopedic injuries^{7,8}.

While extravasated whole blood is rapidly cleared out by the barrier functions of the synovial membrane, even singular bleeding episode has been demonstrated to initiate the inflammatory cascade leading to downstream tissue changes such as hyperplasia and neoangiogenesis through the development of hemosiderotic synovium.^{2,9} Furthermore, *in vivo* preclinical canine models of acute joint bleeds as well as *ex vivo* analyses of blood-affected human cartilage have revealed rapid and irreversible changes to cartilage and synovium that are representative of early-stage osteoarthritis.^{10,11} Blood-induced tissue changes include collagen (COL) loss and proteoglycan release from the cartilage extracellular matrix (ECM) as well as evidence of synovial filtration failure such as the presence of hemosiderin deposits and the upregulation of iron regulators (e.g., ferroportin, heme carrier protein-1). In addition, the pro-inflammatory changes to synovial tissue architecture include pannus formation, hypertrophy, and villous proliferation as evidenced by histopathological staining^{12,13}. Inflamed synovium is highly productive in a feed-forward manner and further contributes to maintaining a pro-inflammatory environment through the production of cytokines, proangiogenic factors, matrix degradation enzymes, as well as immune cell-recruiting chemokines¹⁴. While the broader catabolic tissue changes due to whole blood exposure have been well documented, the mechanisms by which individual blood components drive them are yet to be fully elucidated. As such, previous research has aimed to identify the specific contributions of whole blood factors through direct and indirect interactions with joint tissues, such as through modulation of paracrine factors^{5,15,16}.

Intraarticular iron is of particular interest due to its key roles in cellular regulatory cycles and its capacity to produce free hydroxyl radicals in the presence of hydrogen peroxide, which is upregulated by chondrocytes following blood exposure^{17–20}. These broad spectrum reactive oxygen species (ROS) have been implicated in blood-induced chondrocyte death through caspase activation leading to chondrocyte apoptosis^{15,21}. In addition, iron-generated ROS, their induction of lipid peroxidation, and the inactivation of glutathione peroxidase 4 have been shown to contribute to osteoarthritis progression independent of joint bleeding via ferroptosis, an iron-dependent form of lytic cell death^{22–24}. Biomarkers for both of these cell death mechanisms, including caspase activation and lipid peroxidation for apoptosis and ferroptosis, respectively, have been identified in clinical osteoarthritic samples of human cartilage and synovial fluid. These distinct cell fates may serve as parallel pathways following blood exposure that lead to common tissue-level osteoarthritic features that have been observed following hemarthrosis^{25–27}.

The studies presented here build on previously reported mechanisms of chondrocyte death following iron and whole blood treatment and assess in depth, the specific contributions of red blood cells (RBCs) on cartilage in the context of pro-ferroptotic mechanisms in hemophilic arthropathy (Fig. 1). First, the direct cellular effects of intact RBCs (RBC_{INT}) were assessed in an *in vitro* model of hemophilic arthropathy using human chondrocyte-generated tissue-engineered cartilage (Study 1)^{28,29}. Key results from Study 1 indicated loss of cartilage biochemical and mechanical properties without parallel decreases to DNA content following RBC_{INT} treatment. As such, it was hypothesized that RBC_{INT}

treatment induces nonlethal chondrocyte mechanisms via soluble paracrine factors that increase susceptibility to tissue deterioration while intracellular RBC components such as iron induce direct lethal responses in chondrocytes, given previously published reports on the toxicity of iron-generated ROS^{30–32}. Because RBCs are both sources of inflammatory cytokines and stimulatory soluble factors as well as key transporters of iron, isolated chondrocyte monolayers were treated with both RBC_{INT} (Study 2) as well as red blood cell lysates (RBC_{LYS}) (Study 3) to elucidate their individual contributions to chondrocyte damage. Both intact RBCs and RBC lysates were included in this investigation, as both blood and blood components are implicated in blood-induced joint damage and rationale for the latter is further supported by the presence of hemosiderotic synovium following hemarthrosis cases in both hemophilic and non-hemophilic patients^{2,13,33,34}. Furthermore, RBCs are subject to releasing up to 2.5×10^8 molecules of hemoglobin per cell upon senescence or lysis due to physical and cellular insults, leading to potential cartilage toxicity driven by intracellular iron^{35,36}. We directly link blood components to ROS-mediated and ferroptotic mechanisms and demonstrate the multimodal nature of RBC-induced damage to cartilage that contributes to the clinically-observed features of hemophilic arthropathy. Ferrostatin-1, a radical trapping lipophilic antioxidant, was also assessed for its therapeutic potential in mitigating cellular damage driven by RBC-, and subsequently, iron exposure³⁷. It was hypothesized that RBCs, as well as their intracellular components, are contributors to the cartilage damage observed in patients with hemophilic arthropathy. A deeper mechanistic understanding of RBC-induced chondrocyte death will inform novel therapeutic targets and strategies for patients suffering from this condition. Moreover, these studies may have implications on ameliorating the contribution of joint bleeding on the development of post-traumatic osteoarthritis.

Methods

Materials and reagents

Dulbecco's modified Eagle medium (DMEM, Product No. 11965092), human fibroblast growth factor-2 (FGF-2, Product No. PHG0026), transforming growth factor beta-1 (TGFβ-1, Product No. PHG9214), antibiotic-antimycotic (A/A, Product No. 15240062), MitoSOX mitochondrial superoxide indicator (Product No. M36008), and BODIPY 581/591 C11 (Product No. D3861) were purchased from ThermoFisher Scientific. Type VII agarose (Product No. A4018), L-proline (Product No. P5607), L-ascorbic acid (Product No. A8960), sodium pyruvate (Product No. S8636), dexamethasone (Product No. D4902), 1S,3R-RSL3 (RSL3, Product No. SML2245), and Ferrostatin-1 (Product No. SML0583) were purchased from Sigma-Aldrich. Fetal bovine serum (FBS, Product No. S11150) and transforming growth factor beta-3 (TGFβ-3, Product No. 243B3200) were purchased from R&D Systems.

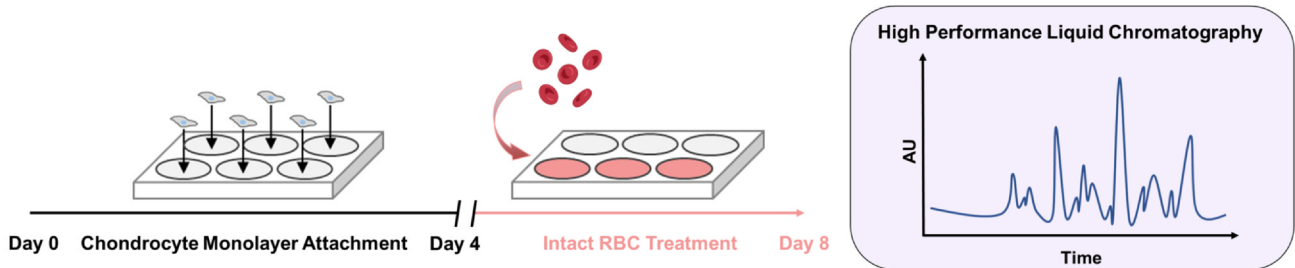
Chondrocyte isolation and culture

Human cartilage grafts were obtained from MTF Biologics (Edison, NJ) following allograft expiration and from a deceased donor (NDRI Protocol #RHUC1-01) (Table 1). Primary chondrocytes were isolated by digesting cartilage pieces in type II collagenase for 16 h at 37 °C and were subsequently cultured in DMEM supplemented with 10% FBS, 1% A/A, 5 ng/mL FGF-2, and 1 ng/mL TGFβ-1. All cells were used between passage 1 and passage 4, as loss of chondrogenic phenotype has been observed beyond passage 5³⁸. All experiments were conducted in serum-free chemically-defined media (CM), consisting of DMEM supplemented with 1% insulin-transferrin-selenium, 100 μg/mL sodium pyruvate, 50 μg/mL L-

Study 1: *In Vitro* model of hemarthrosis using human chondrocyte-based tissue engineered cartilage



Study 2: Effect of intact RBC (RBC_{INT}) on human chondrocyte monolayers



Study 3: Effect of RBC lysates (RBC_{LYS}) on human chondrocyte monolayers

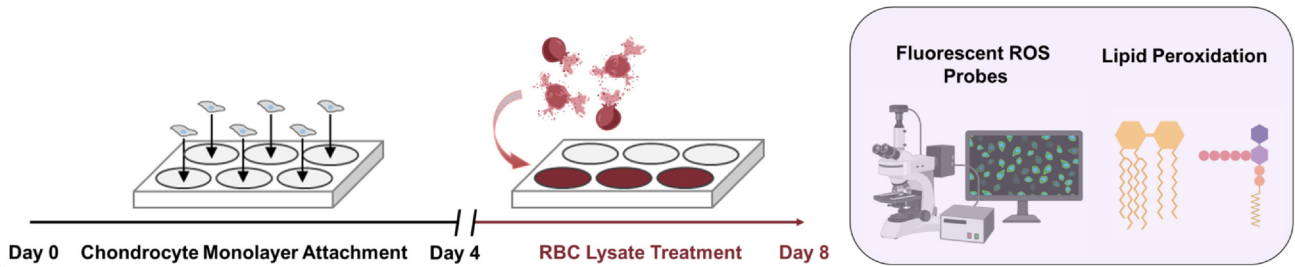


Fig. 1

Overview of experimental designs.

Donor	Age	Sex	Donor tissue source	Cartilage condition	Notable comorbidity	Used in study #
D1	17	Male	Expired graft (MTF Biologics)	Healthy	None	Study 1, 2
D2	31	Male	Expired graft (MTF Biologics)	Healthy	None	Study 2, 3
D3	35	Male	Expired graft (MTF Biologics)	Healthy	None	Study 2
D4	39	Male	Deceased donor (NDRI)	Healthy	Scleroderma	Native tissue validation

Table 1

Donor information and allocation in outlined studies

proline, 1% A/A, 5 ng/mL FGF-2, and 1 ng/mL TGF β -1 to maintain chondrogenic phenotype.

RBC isolation and lysate formation

O⁺ leukocyte-reduced whole human blood was purchased from the New York Blood Center for each separate study and used no later than 2 days postcollection. Blood from one new donor was used for each study. Erythrocytes were separated using the Ficoll-Paque technique and purified by three cycles of washing and centrifugation at 800 \times g with cold Phosphate Buffered Saline (PBS). Isolated RBCs were lysed to extract intracellular blood components as previously described³⁹. RBC lysates were either used fresh for experiments or frozen at -80°C for future use. Fresh intact RBCs were applied on day of treatment.

Engineered cartilage responses to RBC treatment (Study 1)

Chondrocytes from donor D1 were seeded in 2% agarose hydrogel sheets at a density of 30×10^6 cells/mL and cylindrical engineered cartilage constructs were formed using sterile 4 mm biopsy punches. Constructs were cultured to maturity for 28 days in CM supplemented with 50 $\mu\text{g/mL}$ L-ascorbic acid, 100 nM dexamethasone, and 10 ng/mL TGF β -3 as previously described²⁸. Engineered constructs were treated with CM \pm 20% (v/v) RBC_{INT} for 4 days (N=5 control, N=6 RBC_{INT}) and assessed for changes in mechanical and biochemical properties. Following experimental treatment, samples were weighed, frozen overnight at -20°C , and subsequently lyophilized for 48 h until completely dry at -50°C . Sample dry weights (DW) were measured prior to proteinase K digestion (0.5 mg/mL in proteinase K buffer) for 16 h. The biochemical compositions of cartilage tissues were determined through measurements of glycosaminoglycans (GAG), COL, and DNA using the dimethylmethylene blue, orthohydroxyproline, and PicoGreen assays, respectively. DNA was normalized to sample DW and GAG and COL content were normalized to sample DNA to reflect cellular production. Engineered cartilage constructs were also assessed for changes to equilibrium and dynamic moduli as well as markers of tissue breakdown (e.g., Media GAG and nitric oxide production by Griess Assay), which were normalized to construct volumes.

Chondrocyte viability in response to RBC treatment

Chondrocytes from donor D1 were plated on glass bottom dishes at a density of 50,000 cells per well and allowed to attach and proliferate for 24 h in culture media. On the day of treatment, culture media was removed and cells were washed twice with fresh PBS. Chondrocyte monolayers (N = 4/treatment) were cultured for 48 h in CM + 0, 6.3, 12.5, 20%, or 25% (v/v) of either RBC_{INT} or RBC_{LYS} and assessed for viability using 2 μM Calcein-AM and 4 μM ethidium homodimer-1 as indicators of live and dead cells, respectively. Based on viability results, it was deemed that 20% (v/v) was the minimum concentration of lysates to induce significantly greater toxicity than intact RBCs and was used for subsequent lipidomics analyses and measures of oxidative stress.

Intracellular changes to chondrocytes following treatment with RBC_{INT} (Study 2)

Blood-induced changes to chondrocyte monolayers were assessed in more depth via metabolomic analysis of chondrocyte lysates. Chondrocyte monolayers from donors D1, D2, and D3 were treated with CM or CM + 20% RBC_{INT} (v/v) \pm 10 μM Ferrostatin-1 for 48 h and subsequently lysed to isolate intracellular lipids by phase separation. A monolayer from each independent donor was treated

under each condition. Isolated lipids were analyzed on an Acquity UPLC I-Class chromatograph coupled to a high-resolution quadrupole time-of-flight mass spectrophotometer, Synapt G2 and identified using the metabolite mass spectral database, METLIN^{40,41}.

Assessment of ROS-mediated mechanisms following RBC_{LYS} treatment (Study 3)

The production of mitochondrial superoxides was assessed by MitoSOX staining of chondrocyte monolayers from donor D2 treated with CM + 20% (v/v) RBC_{LYS} or an equivalent concentration of solubilized ferric ammonium citrate \pm 10 μM Ferrostatin-1. Cells were counterstained using Hoescht 33342 dye according to manufacturer-recommended dilutions. To assess chondrocyte lipid peroxidation, near-confluent chondrocyte monolayers from the same donor were treated with CM + 20% (v/v) RBC_{LYS} \pm 10 μM Ferrostatin-1. Fluorescent visualization and quantification of lipid peroxidation were conducted using a BODIPY C-11^{581/591} probe by taking the relative fluorescence emission peaks at $\lambda_{\text{EX}} = 590$ nm and $\lambda_{\text{EX}} = 510$ nm for individual cells. The ferroptosis inducer, RSL3 (2 μM), was applied as a positive control for the lipid peroxidation probe.

Cross-validation in native human explants

Native cartilage explants from donor D4 were treated with 20% (v/v) RBC_{INT} \pm 10 μM Ferrostatin-1 for 4 days and assessed for changes in mechanical and biochemical properties as was conducted for tissue-engineered cartilage in Study 1. The production of mitochondrial superoxides was further confirmed by MitoSOX staining of superficial layer cartilage taken from three different regions following treatment with CM + 20% (v/v) RBC_{LYS} \pm 10 μM Ferrostatin-1 as described in Study 3.

Statistical analyses

Data were checked for normality using the Shapiro-Wilk test and for homoscedasticity. Heteroscedastic data were log-transformed prior to statistical analysis. Differences in construct and explant properties, as well as cell viability and lipid peroxidation were determined using a Student's t-test for equal variances and Welch's t-test for unequal variances or one-way ANOVA followed by Tukey's posthoc test for multiple comparisons. Data are presented in figures as mean \pm standard deviation (SD), and reported in the text as the 95% confidence intervals (CI) for the differences of means. Lipid signal intensities were log-transformed and analyzed using Friedman's test followed by Dunn's correction for multiple comparisons. Data are presented as median \pm 95% CI. Statistical analyses were performed on R (R Core Team, 2019) and GraphPad Prism 9.0 ($\alpha < 0.05$).

Results

Intact RBC-induced changes to engineered cartilage (Study 1)

Engineered cartilage constructs following experimental treatment were statistically similar in diameter (RBC_{INT} vs. Control 95% CI: [-0.0966, 0.1946], $P = 0.4659$), although height was decreased following intact RBC exposure (RBC_{INT} vs. Control 95% CI: [-0.1162, -0.0078], $P = 0.0293$) (Fig. 2A). DNA content was not significantly decreased in cartilage constructs treated with intact RBCs (RBC_{INT} vs. Control 95% CI: [-194.6, 123.9], $P = 0.6279$). Similarly, quantification of matrix components, GAG (RBC_{INT} vs. Control 95% CI: [-0.0739, 0.1936], $P = 0.3379$) and COL (RBC_{INT} vs. Control 95% CI: [-0.0058, 0.0011], $P = 0.1497$) were not statistically different in both control and experimentally treated constructs (Fig. 2B). However,

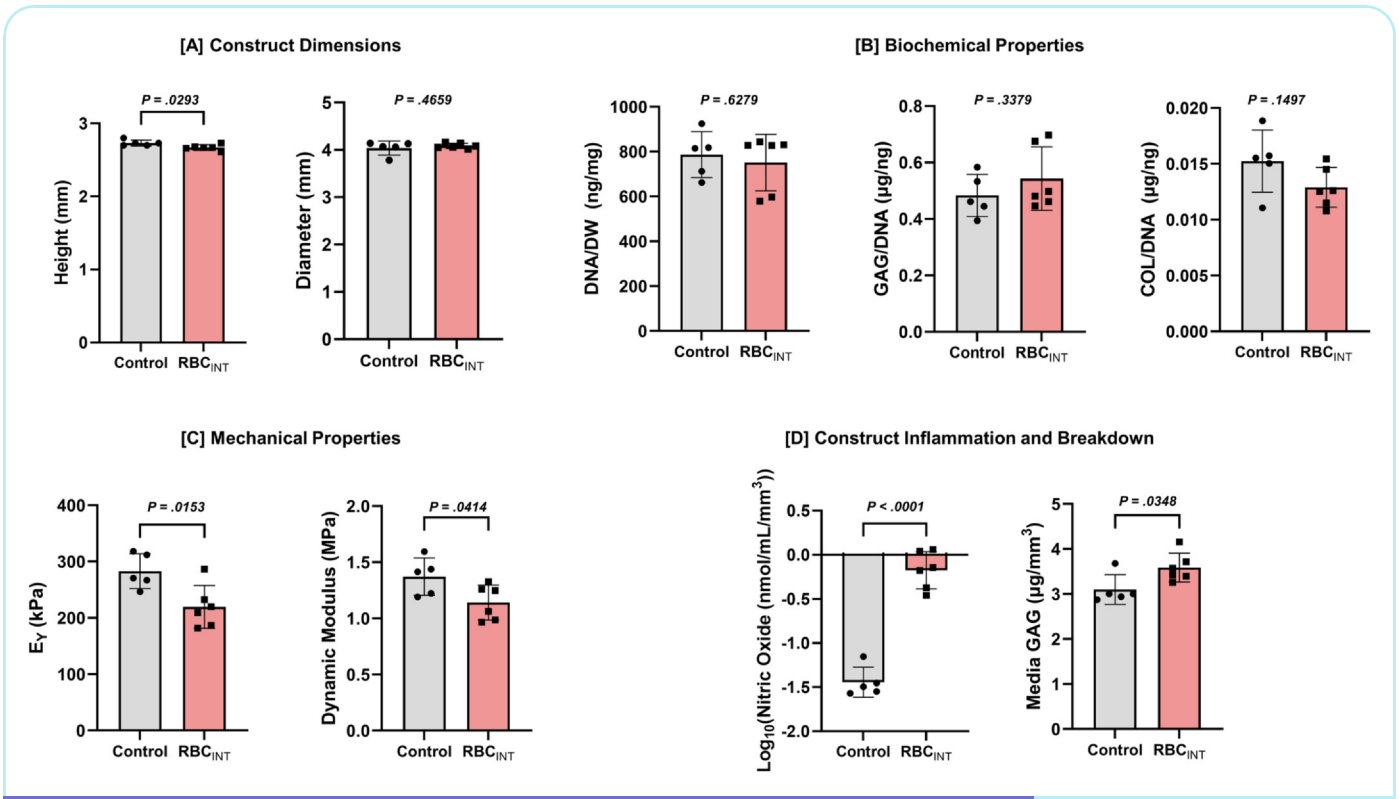


Fig. 2

Osteoarthritis and Cartilage

Changes to tissue-engineered cartilage constructs following RBC_{INT} treatment. Tissues were assessed for changes to (A) physical changes, (B) biochemical and (C) mechanical properties, as well as for (D) evidence of tissue deterioration. Bars represent mean ± SD.

measurements of cartilage breakdown and mechanical properties were significantly changed in RBC_{INT}-treated constructs. The mechanical properties of cartilage constructs were significantly decreased following intact RBC treatment, as measured by both Young's modulus (RBC_{INT} vs. Control 95% CI: [-111.4, -15.39], $P=0.0153$) and dynamic modulus (RBC_{INT} vs. Control 95% CI:

[-0.4497, -0.0112], $P=0.0414$) (Fig. 2C). Both the production of nitric oxide (RBC_{INT} vs. Control 95% CI: [0.3541, 1.034], $P < 0.0001$) and release of GAG (RBC_{INT} vs. Control 95% CI: [0.0434, 0.9317], $P=0.0348$) into the culture media were significantly elevated in RBC_{INT}-treated constructs, indicating statistically significant catabolic and pro-inflammatory tissues to RBC-treated tissues (Fig. 2D).

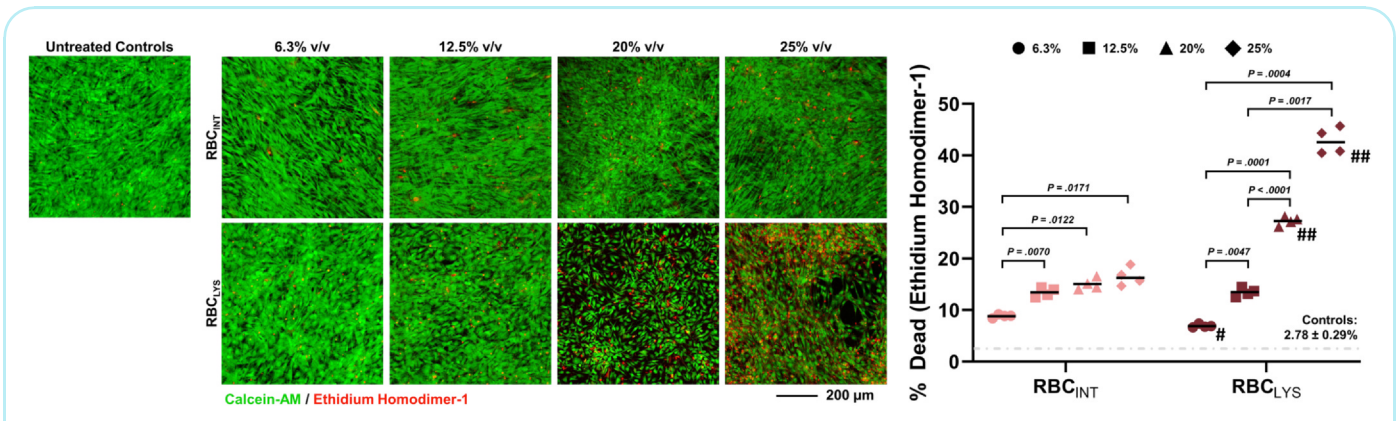


Fig. 3

Osteoarthritis and Cartilage

Assessment of RBC-induced changes to chondrocyte viability. (Left) Confocal imaging of chondrocyte monolayers following treatment with increasing concentrations of RBC_{INT} and RBC_{LYS}. (Right) Quantification of chondrocyte viability following RBC-treatment. Viability was quantified by taking the percentage of ethidium homodimer-1 ($\lambda_{Em} = 617$ nm) intensity with respect to the total fluorescence intensity including Calcein-AM ($\lambda_{Em} = 517$ nm). Bars represent mean ± SD. # $P < 0.001$, ## $P < 0.0001$ between RBC_{INT} and RBC_{LYS}.

Loss of chondrocyte viability depends on RBC integrity

Chondrocyte monolayers exhibited a significant dose-dependent loss of viability following both RBC_{INT} and RBC_{LYS} treatment as quantified by taking the ratio of the ethidium homodimer-1 ($\lambda_{Em} = 617$ nm) channel to the total fluorescence intensity including Calcein-AM ($\lambda_{Em} = 517$ nm) (Fig. 3). However, those treated with RBC lysates exhibited a significantly lower viability at 25% than their intact counterparts, indicating differential responses of chondrocytes to intact RBCs perhaps due to their secreted factors, and to intracellular RBC lysates such as iron.

Metabolomic changes to chondrocytes following RBC_{INT} treatment (Study 2)

Lipidomic analysis of chondrocytes following RBC treatment demonstrated widespread increases in fatty acids (FA), phosphatidylcholines (PC), phosphatidylethanolamine (PE), phosphatidylglycerol (PG), ceramides (Cer), and hexosylceramides (HexCer), which were mitigated by the addition of Ferrostatin-1 (Fig. 4A). The chromatography signal intensities of selected lipid species that have been demonstrated to contribute to chondrocyte pathology were found to be significantly elevated in blood-treated groups (Fig. 4B).

RBC_{LYS} treatment of chondrocytes induces changes representative of ferroptosis (Study 3)

Intracellular lipid peroxidation was probed using the BODIPY C-11^{581/591} dye according to manufacturer instructions. A ferroptosis-inducer, RSL3, was used as a positive control for the probe. The relative fluorescence intensity of the FITC ($\lambda = 510$ nm) channel compared to the Texas Red ($\lambda = 590$ nm) channel was quantified as a measure of relative oxidation. Chondrocytes treated with RSL3 exhibited significantly higher oxidation than all other groups ($P < 0.0001$) and confirmed proper assay function. RBC_{LYS} treatment induced a significantly increased oxidation state in chondrocytes, which was mitigated by Ferrostatin-1 treatment ($P < 0.0001$) (Fig. 5A). The production of mitochondrial reactive oxygen species (mROS) was also assessed in RBC_{LYS}- and iron-treated chondrocytes. Both ferric iron and RBC lysates induced production of mROS as well as mitochondrial fragmentation, which were reduced with Ferrostatin-1 (Fig. 5B).

Validation of biochemical changes and mitochondrial ROS production in native cartilage

DNA content was not statistically different in human cartilage explants treated with RBC_{INT} compared to those treated with RBC_{INT} + Ferrostatin-1 (RBC_{INT} vs. RBC_{INT} + Ferrostatin-1 95% CI: [-2.616, 134.3], $P = 0.0595$) or under control conditions (RBC_{INT} vs. Control 95% CI: [-28.13, 121.9], $P = 0.2507$). GAG was significantly reduced in RBC_{INT}-treated explants compared to control (RBC_{INT} vs. Control 95% CI: [-0.3513, -0.0138], $P = 0.0262$), and Ferrostatin-1 treatment demonstrated an opposite trend (RBC_{INT} vs. RBC_{INT} + Ferrostatin-1 95% CI: [-0.2809, 0.0272], $P = 0.1102$). COL decreased, though not significantly in RBC_{INT}-treated explants compared to control (RBC_{INT} vs. Control 95% CI: [-1.619, 0.2160], $P = 0.1419$), while Ferrostatin-1 treatment significantly elevated normalized COL content (RBC_{INT} vs. RBC_{INT} + Ferrostatin-1 95% CI: [-1.944, -0.2691], $P = 0.0088$) (Fig. 6A). Mitochondrial ROS production, as visualized with MitoSOX staining, was also elevated in RBC_{LYS}-treated cartilage explants compared to their control and Ferrostatin-1-treated counterparts (Fig. 6B).

Discussion

Hemarthrosis of the knee is clinically observed in both traumatic (e.g., joint injury and surgery) and nontraumatic (e.g., hemophilia) cases, wherein the management of joint bleeds especially has been a subject of debate, especially in postoperative hemarthrosis. Mechanisms of joint damage following both singular and repeated cases of hemarthrosis, such as the loss of cartilage GAG and the formation of hypertrophic synovium have been implicated in the long-term degenerative changes to the joint space and in the contribution to the development of post-traumatic osteoarthritis in patients who undergo routine orthopedic procedures^{8,42}. However, the cellular mechanisms that may contribute to the development of hemophilic arthropathy following blood exposure to the joint are yet to be fully elucidated. To this end, the harmful effects of blood- and iron-exposure on joint health have been broadly explored in vitro as well as in vivo using both human tissues and canine models^{5,11,15,43–47}. Iron is widely implicated in osteoarthritis progression and synovial iron deposition is a common feature in hemophilic patients³⁰. Synovium from hemophiliacs demonstrate significantly elevated production of pro-inflammatory cytokines, and targeting of their receptors has been studied as potential therapies for hemophilic arthropathy^{30,44,48}. In addition, lipid peroxidation end-products in the synovial fluid of osteoarthritis patients and their catabolic changes to cartilage ECM have been reported in the synovial fluid of osteoarthritic patients^{26,27,49}. To expand on the results of previously published results, we sought to explore the specific modulatory effects of RBCs in an in vitro human-tissue based model of hemophilic arthropathy.

First, the loss of functional properties of cartilage was confirmed following exposure to intact RBCs through measurements of biochemical content, mechanical properties, and tissue inflammation and integrity. Interestingly, decreases in ECM content and mechanical properties, as well as a stronger inflammatory response without parallel loss of tissue cellularity, were observed in cartilage tissues, suggesting a shift in the anabolic and catabolic activities following intact RBC exposure. This may be attributed to the paracrine signaling capacity of RBCs through pro-inflammatory cytokines and other soluble factors that drive pro-catabolic pathways, which is supported by recent work by Karsten and colleagues, wherein conditioned media generated from intact RBCs consisted of considerable pro-inflammatory soluble factors³². Pro-catabolic changes to chondrocytes following blood exposure were also observed in our cultures, through downregulated gene expression of aggrecan, COL type II, interleukin-10, combined with upregulation of matrix metalloproteinase-14, which is involved in tissue turnover and elevated disease-states⁵⁰.

In monolayer culture, greater cell toxicity was observed in chondrocyte monolayers treated with RBC lysates than their intact counterparts, and as such, the nonlethal modulatory role of intact RBCs was examined through metabolomic analyses of chondrocyte lipid profiles in the context of ferroptosis. Lipids are key players in ferroptosis and assessments of cellular lipid profiles have been widely used as indicators of cellular state in both primary cell monolayers and three-dimensional pellets^{51,52}. Ceramides at high concentrations are implicated in downregulation of type II COL by shifting the homeostatic balance toward matrix catabolism⁵³. FAs are the principal offenders in lipotoxicity and apoptosis induction in articular cartilage. FA 18:2 is highly oxidizable and has been shown to directly affect COL ratios in cardiac muscle as well as to indirectly modulate neurotransmission following ischemic brain injury through its metabolites^{54–56}. Our assessment of lipid profiles in RBC-affected chondrocytes revealed significant increases in a variety of FAs, ceramides, as well as phosphatidylcholines, -ethanolamines, and -glycerol. As such, the detrimental effects of erythrocyte

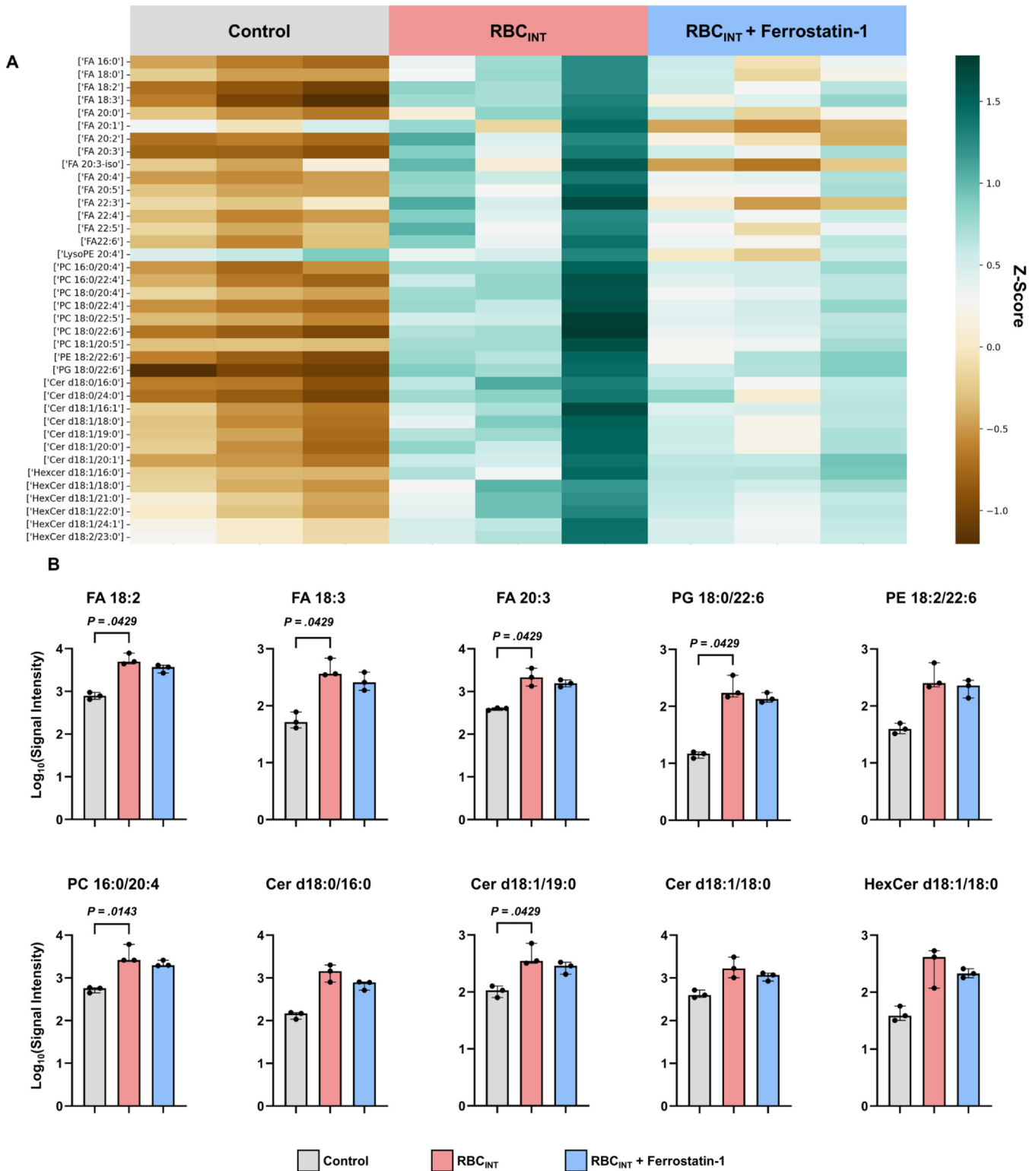


Fig. 4

(A) Heatmap of significantly elevated lipid species in chondrocytes in responses to RBC_{INT} treatment and mitigation by Ferrostatin-1. Each row represents the detected lipid species. Each column represents a sample. The relative abundance of each lipid is color-coded, with blue indicating high signal intensity and brown indicating low signal intensity. (B) Liquid chromatography - mass spectrometry (LC-MS) signal intensities of selected lipid species. Bars represent median ± 95% CI. FA: Free fatty acid; PC: phosphatidylcholine; PE: phosphatidylethanolamine; PG: phosphatidylglycerol; Cer: ceramide; HexCer: HexosylCer.

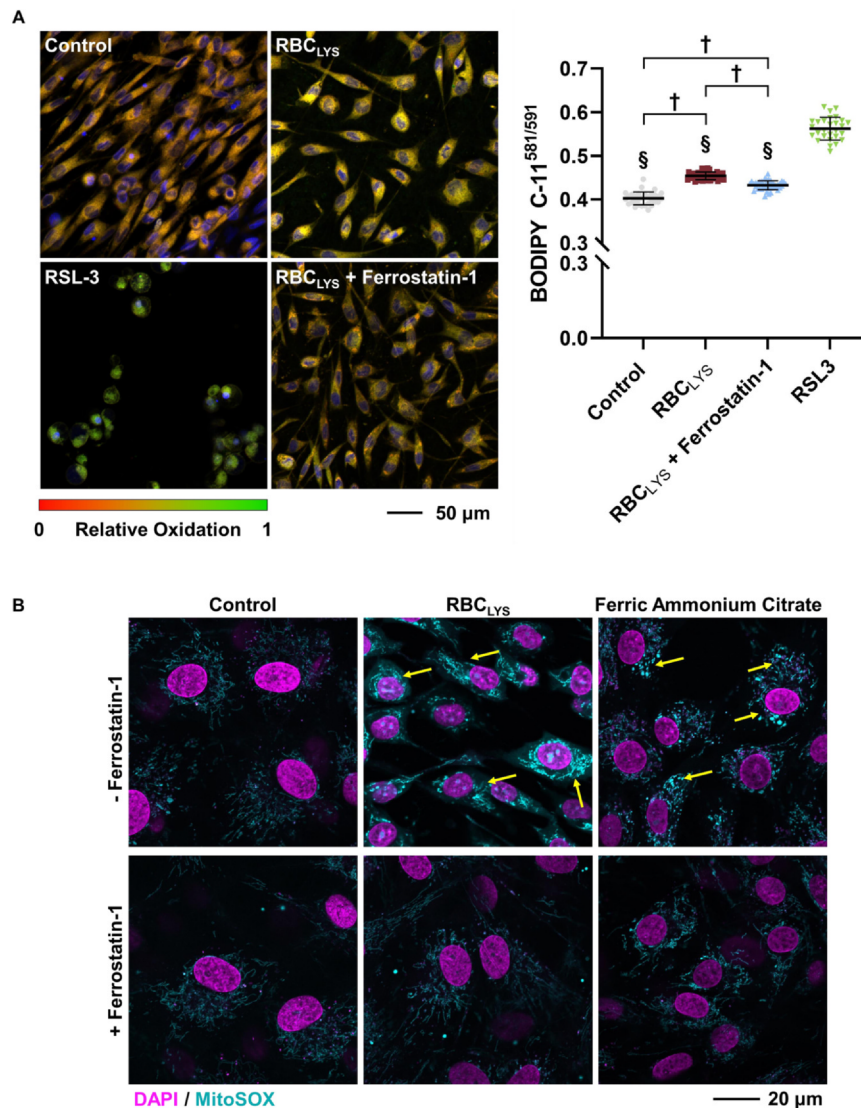


Fig. 5

(A) Lipid peroxidation induced by RBC_{LYS} measured by the BODIPY C-11^{581/591} probe using the ferroptosis inducer, RSL3, as a positive control. The ratios of the intensity of oxidized undecanoic acid (Ex/Em: 488/510 nm) to the intensity of reduced undecanoic acid (Ex/Em: 581/591 nm) were measured for individual cells (N = 28–44 cells). [†]*P* < 0.0001. [§]*P* < 0.0001 vs. RSL3. (B) Visualization of mitochondrial superoxides in response to iron and RBC_{LYS} treatment and assessment of the therapeutic capacity of Ferrostatin-1. Yellow arrows indicate presence of mitochondrial superoxides induced by RBC_{LYS} and iron treatment.

exposure on chondrocytes may be two-fold: an indirect toxicity from paracrine factors secreted by intact RBCs that shifts the cellular profile toward one that is more susceptible to oxidation and matrix degradation, as well as a direct loss of cell viability in response to RBC lysates such as iron.

The direct, pro-inflammatory, and cytotoxic functions of intracellular RBC components, particularly iron, were further assessed through treatment of chondrocytes with RBC lysates in Study 3. Increased lipid peroxidation and mitochondrial ROS expression were observed in chondrocytes treated with iron and RBC lysates compared to control, implicating the potential role of ferroptosis in RBC-exposed cartilage. Ferroptosis has been previously shown to contribute to osteoarthritis progression following treatment with IL1 β - and ferric ammonium citrate treatment in both isolated murine

chondrocytes as well as in an in vivo destabilized medial meniscus-induced osteoarthritis model, with rescue by Ferrostatin-1²³. Treatment with Ferrostatin-1 in our assessments also demonstrated similar therapeutic capabilities by protecting chondrocytes and cartilage against detrimental changes to lipid profiles as well as ROS production and lipid peroxidation. The results from this present study expand the pro-ferroptotic findings in the murine model to human chondrocytes as well as native human cartilage explants and demonstrate the direct contribution of erythrocytes on chondrocyte death on multiple fronts. As such, we accept the hypothesis that both intact and lysed RBCs are contributors to the cartilage damage observed following hemarthrosis.

However, there are a few limitations, one of which was the lack of available autologous blood for all studies and as a result, separate

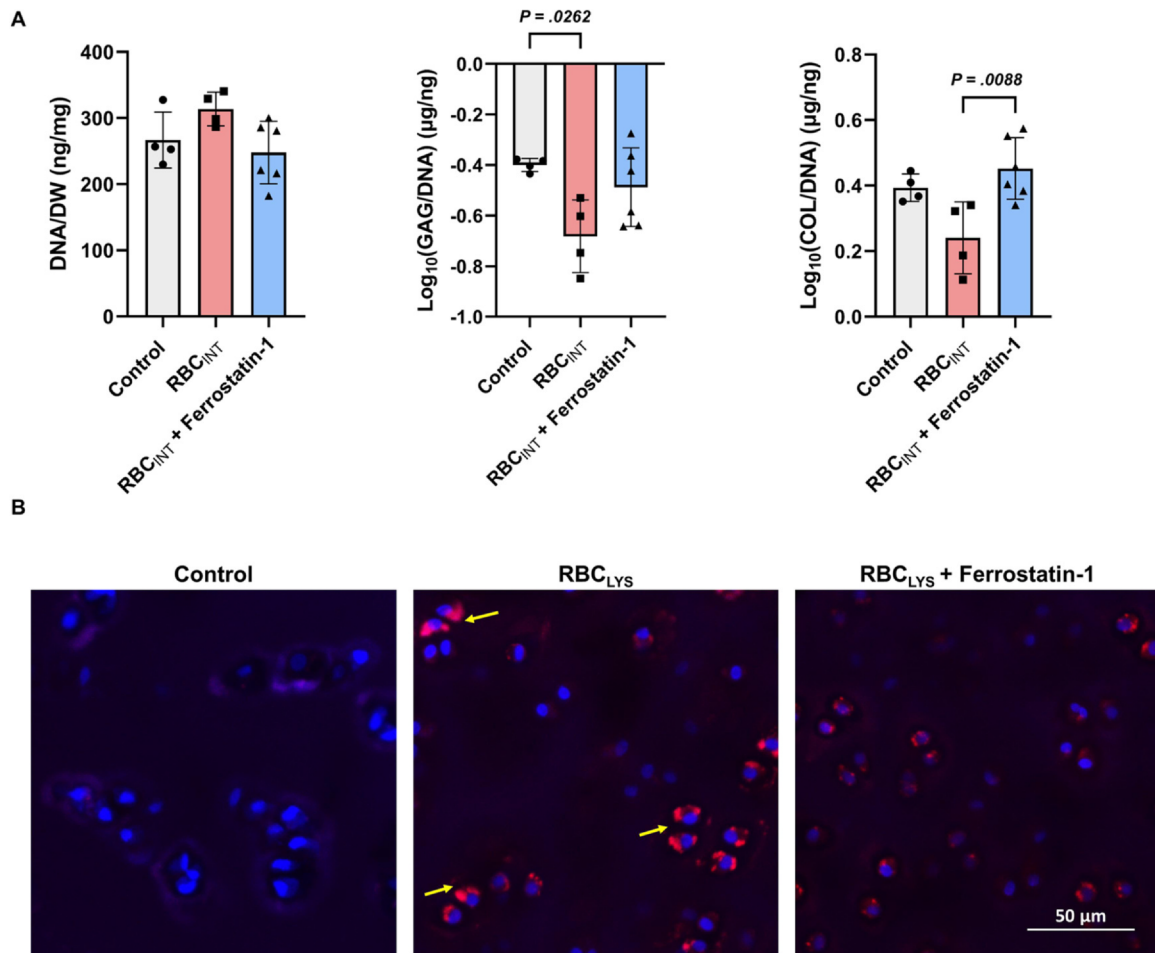


Fig. 6

(A) Changes to the DNA, GAG, and COL content of native cartilage explants following RBC_{INT} treatment and 10 µM Ferrostatin-1. Bars represent mean ± SD. (B) MitoSOX staining for mitochondrial superoxides (yellow arrows) in human cartilage explants treated with RBC_{LYS} ± 10 µM Ferrostatin-1.

batches of homologous blood were used for studies 1–3. However, autologous blood was used in the validation using human explant cartilage and resulted in similar trends as tissue-engineered cartilage treated with homologous blood. These results were in agreement with previously published literature using both autologous and homologous blood in an in vivo canine and in an in vitro human model of blood-induced joint damage^{45,57,58}. In addition, while the studies described here were validated against human explants from a single healthy donor, they employed human-based engineered cartilage and chondrocytes, and are limited by the lack of clinical controls (e.g., explants from patients with hemophilic arthropathy). Studies 2 and 3 were only performed on chondrocyte monolayers due to technical difficulties in isolating chondrocytes from agarose hydrogels and will be further explored to expand these findings to 3D culture systems. While we performed four different in vitro experimental studies, utilizing an aggregate of four cartilage donors and four blood donors, which consistently demonstrated ferroptotic mechanisms in blood-mediated chondrocyte cell death, the paucity of available human cells and tissues is a major limitation. Studies 1,

3, and 4 were conducted using only one biological replicate and Study 2 incorporated three donors, and as such, these results are subject to variance in the underlying population as well as variability in the interactions between cartilage–blood donor pairings. Future studies will aim to increase the number of cartilage donors, strategically administer Ferrostatin-1 during a therapeutic window following a joint bleed, and optimize concentrations through dose–response studies. This can potentially be done through the sustained release of therapeutics as previously described by us and others, and as is employed in the clinic for treatment of joint diseases such as osteoarthritis^{59–62}.

Role of the Funding Source

A.J.L. was supported by NIH 5F31AR078004. Research materials for A.J.L., L.R.G., F.Z., and C.T.H. were purchased through NIH 5P41EB027062 and SEAS Interdisciplinary Research Seed (SIRS) Funding through Columbia University. This research of B.R.S. was supported by NCI/NIH R35CA209896.

CRedit authorship contribution statement

Concept and Design: A.J.L., L.R.G. Collection and Assembly of data: A.J.L., L.R.G., F.Z. Analysis and Interpretation of data: A.J.L., L.R.G., F.Z. Drafting of the article: A.J.L., L.R.G. Critical revision and Final approval: A.J.L., L.R.G., F.Z., B.R.S., C.T.H. Obtaining of Funding: A.J.L., B.R.S., C.T.H.

Conflict of Interest

A.J.L., L.R.G., F.Z., and C.T.H. have nothing to disclose. B.R.S. is an inventor on patents and patent applications involving small molecule drug discovery and ferroptosis; has co-founded and serves as a consultant to Inzen Therapeutics, Exarta Therapeutics, and ProJenX, Inc.; serves as a consultant to Weatherwax Biotechnologies Corporation and Akin Gump Strauss Hauer & Feld LLP; and receives sponsored research support from Sumitomo Dainippon Pharma Oncology.

Acknowledgements

The authors would like to thank the mass spectrometry facility at Columbia University for assisting with the acquisition and interpretation of metabolomics data as well as MTF Biologics for providing tissue grafts.

References

- Wilkins RA, Stephensen D, Siddle H, Scott MJ, Xiang H, Horn E, et al. Twelve-month prevalence of haemarthrosis and joint disease using the Haemophilia Joint Health score: evaluation of the UK National Haemophilia Database and Haemtrack patient reported data: an observational study. *BMJ Open* 2022;12(1), e052358. <https://doi.org/10.1136/bmjopen-2021-052358>
- Lyons LP, Weinberg JB, Wittstein JR, McNulty AL. Blood in the joint: effects of hemarthrosis on meniscus health and repair techniques. *Osteoarthr Cartil* 2021;29(4):471–9. <https://doi.org/10.1016/j.joca.2020.11.008>
- Branam GM, Saber AY. Osteochondral Autograft Transplantation. *StatPearls*. StatPearls Publishing.; 2022 Accessed March 13, 2023 (<http://www.ncbi.nlm.nih.gov/books/NBK560655/>).
- Camillieri G, Margheritini F, Maresca G, Mariani PP. Postoperative bleeding following notchplasty in anterior cruciate ligament reconstruction: thermal radio frequency versus powered instrumentation. *Knee Surg Sports Traumatol Arthrosc* 2001;9(1):12–4. <https://doi.org/10.1007/s001670000176>
- van Meegeren MER, Roosendaal G, Jansen NWD, Lafaber FPJG, Mastbergen SC. Blood-induced joint damage: the devastating effects of acute joint bleeds versus micro-bleeds. *Cartilage* 2013;4(4):313–20. <https://doi.org/10.1177/1947603513497569>
- Myers SL, Brandt KD, O'Connor BL, Visco DM, Albrecht ME. Synovitis and osteoarthritic changes in canine articular cartilage after anterior cruciate ligament transection. Effect of surgical hemostasis. *Arthritis Rheum* 1990;33(9):1406–15. <https://doi.org/10.1002/art.1780330913>
- Cheung EC, DiLallo M, Feeley BT, Lansdown DA. Osteoarthritis and ACL reconstruction—myths and risks. *Curr Rev Musculoskelet Med* 2020;13(1):115–22. <https://doi.org/10.1007/s12178-019-09596-w>
- Magarian EM, Fleming BC, Harrison SL, Mastrangelo AN, Badger GJ, Murray MM. Delay of 2 or 6 weeks adversely affects the functional outcome of augmented primary repair of the porcine anterior cruciate ligament. *Am J Sports Med* 2010;38(12):2528–34. <https://doi.org/10.1177/0363546510377416>
- van Vulpen LFD, van Meegeren MER, Roosendaal G, Jansen NWD, van Laar JM, Schutgens REG, et al. Biochemical markers of joint tissue damage increase shortly after a joint bleed; an explorative human and canine in vivo study. *Osteoarthr Cartil* 2015;23(1):63–9. <https://doi.org/10.1016/j.joca.2014.09.008>
- Jansen NWD, Roosendaal G, Wenting MJG, Bijlsma JWJ, Theobald M, Hazewinkel HAW, et al. Very rapid clearance after a joint bleed in the canine knee cannot prevent adverse effects on cartilage and synovial tissue. *Osteoarthr Cartil* 2009;17(4):433–40. <https://doi.org/10.1016/j.joca.2008.09.001>
- Jansen NWD, Roosendaal G, Bijlsma JWJ, DeGroot J, Lafaber FPJG. Exposure of human cartilage tissue to low concentrations of blood for a short period of time leads to prolonged cartilage damage: An in vitro study. *Arthritis Rheum* 2007;56(1):199–207. <https://doi.org/10.1002/art.22304>
- Nieuwenhuizen L, Schutgens RE g, van Asbeck BS, Wenting MJ, van Veghel K, Roosendaal G, et al. Identification and expression of iron regulators in human synovium: evidence for upregulation in haemophilic arthropathy compared to rheumatoid arthritis, osteoarthritis, and healthy controls. *Haemophilia* 2013;19(4):e218–27. <https://doi.org/10.1111/hae.12208>
- Roosendaal G, Vianen ME, Wenting MJ, van Rinsum AC, van den Berg HM, Lafaber FP, et al. Iron deposits and catabolic properties of synovial tissue from patients with haemophilia. *J Bone Joint Surg Br* 1998;80(3):540–5. <https://doi.org/10.1302/0301-620x.80b3.7807>
- Øvlisen K, Kristensen AT, Jensen AL, Tranholm M. IL-1 beta, IL-6, KC and MCP-1 are elevated in synovial fluid from haemophilic mice with experimentally induced haemarthrosis. *Haemophilia* 2009;15(3):802–10. <https://doi.org/10.1111/j.1365-2516.2008.01973.x>
- Hooiveld M, Roosendaal G, Wenting M, van den Berg M, Bijlsma J, Lafaber F. Short-term exposure of cartilage to blood results in chondrocyte apoptosis. *Am J Pathol* 2003;162(3):943–51.
- Jansen NWD, Roosendaal G, Lafaber FPJG. Understanding haemophilic arthropathy: an exploration of current open issues. *Br J Haematol* 2008;143(5):632–40. <https://doi.org/10.1111/j.1365-2141.2008.07386.x>
- Wen FQ, Jabbar AA, Chen YX, Kazarian T, Patel DA, Valentino LA. c-myc proto-oncogene expression in hemophilic synovitis: in vitro studies of the effects of iron and ceramide. *Blood* 2002;100(3):912–6. <https://doi.org/10.1182/blood-2002-02-0390>
- Hakobyan N, Kazarian T, Jabbar AA, Jabbar KJ, Valentino LA. Pathobiology of hemophilic synovitis I: overexpression of mdm2 oncogene. *Blood* 2004;104(7):2060–4. <https://doi.org/10.1182/blood-2003-12-4231>
- Bystrom LM, Guzman ML, Rivella S. Iron and reactive oxygen species: friends or foes of cancer cells? *Antioxid Redox Signal* 2014;20(12):1917–24. <https://doi.org/10.1089/ars.2012.5014>
- Tabeian H, Betti BF, dos Santos Cirqueira C, de Vries TJ, Lobbezoo F, ter Linde AV, et al. IL-1β damages fibrocartilage and upregulates MMP-13 expression in fibrochondrocytes in the condyle of the temporomandibular joint. *Int J Mol Sci* 2019;20(9):2260. <https://doi.org/10.3390/ijms20092260>
- Asada S, Fukuda K, Nishisaka F, Matsukawa M, Hamanisi C. Hydrogen peroxide induces apoptosis of chondrocytes; involvement of calcium ion and extracellular signal-regulated protein kinase. *Inflamm Res* 2001;50(1):19–23. <https://doi.org/10.1007/s000110050719>
- Dixon SJ, Lemberg KM, Lamprecht MR, Skouta R, Zaitsev EM, Gleason CE, et al. Ferroptosis: an iron-dependent form of non-apoptotic cell death. *Cell* 2012;149(5):1060–72. <https://doi.org/10.1016/j.cell.2012.03.042>

23. Yao X, Sun K, Yu S, Luo J, Guo J, Lin J, et al. Chondrocyte ferroptosis contribute to the progression of osteoarthritis. *J Orthop Transl* 2021;27:33–43. <https://doi.org/10.1016/j.jot.2020.09.006>
24. Miao Y, Chen Y, Xue F, Liu K, Zhu B, Gao J, et al. Contribution of ferroptosis and GPX4's dual functions to osteoarthritis progression. *EBioMedicine* 2022;76, 103847. <https://doi.org/10.1016/j.ebiom.2022.103847>
25. Hwang HS, Kim HA. Chondrocyte apoptosis in the pathogenesis of osteoarthritis. *Int J Mol Sci* 2015;16(11):26035–54. <https://doi.org/10.3390/ijms161125943>
26. Ostalowska A, Birkner E, Wiecha M, Kasperczyk S, Kasperczyk A, Kapolka D, et al. Lipid peroxidation and antioxidant enzymes in synovial fluid of patients with primary and secondary osteoarthritis of the knee joint. *Osteoarthr Cartil* 2006;14(2):139–45. <https://doi.org/10.1016/j.joca.2005.08.009>
27. Shah R, Raska Jr. K, Tiku ML. The presence of molecular markers of *in vivo* lipid peroxidation in osteoarthritic cartilage: a pathogenic role in osteoarthritis. *Arthritis Rheum* 2005;52(9):2799–807. <https://doi.org/10.1002/art.21239>
28. Mauck RL, Soltz MA, Wang CCB, Wong DD, Chao PHG, Valhmu WB, et al. Functional tissue engineering of articular cartilage through dynamic loading of chondrocyte-seeded agarose gels. *J Biomech Eng* 2000;122(3):252–60. <https://doi.org/10.1115/1.429656>
29. Vunjak-Novakovic G, Obradovic B, Martin I, Bursac PM, Langer R, Freed LE. Dynamic cell seeding of polymer scaffolds for cartilage tissue engineering. *Biotechnol Prog* 1998;14(2):193–202. <https://doi.org/10.1021/bp970120j>
30. Ferreira AV, Duarte TL, Marques S, Costa P, Neves SC, dos Santos T, et al. Iron triggers the early stages of cartilage degeneration *in vitro*: the role of articular chondrocytes. *Osteoarthr Cartil* 2021;3(2), 100145. <https://doi.org/10.1016/j.ocarto.2021.100145>
31. Jing X, Du T, Li T, Yang X, Wang G, Liu X, et al. The detrimental effect of iron on OA chondrocytes: importance of pro-inflammatory cytokines induced iron influx and oxidative stress. *J Cell Mol Med* 2021;25(12):5671. <https://doi.org/10.1111/jcmm.16581>
32. Karsten E, Breen E, Herbert BR. Red blood cells are dynamic reservoirs of cytokines. *Sci Rep* 2018;8(1):3101. <https://doi.org/10.1038/s41598-018-21387-w>
33. Morris CJ, Wainwright AC, Steven MM, Blake DR. The nature of iron deposits in haemophilic synovitis. An immunohistochemical, ultrastructural and X-ray microanalytical study. *Virchows Arch A Pathol Anat Histopathol* 1984;404(1):75–85. <https://doi.org/10.1007/BF00704252>
34. Pulles AE, Mastbergen SC, Schutgens REG, Lafeber FPJG, van Vulpen LFD. Pathophysiology of hemophilic arthropathy and potential targets for therapy. *Pharmacol Res* 2017;115:192–9. <https://doi.org/10.1016/j.phrs.2016.11.032>
35. Sukhbaatar N, Weichhart T. Iron regulation: macrophages in control. *Pharmaceuticals ((Basel))* 2018;11(4):137. <https://doi.org/10.3390/ph11040137>
36. Soares MP, Hamza I. Macrophages and iron metabolism. *Immunity* 2016;44(3):492–504. <https://doi.org/10.1016/j.immuni.2016.02.016>
37. Skouta R, Dixon SJ, Wang J, Dunn DE, Orman M, Shimada K, et al. Ferrostatins inhibit oxidative lipid damage and cell death in diverse disease models. *J Am Chem Soc* 2014;136(12):4551–6. <https://doi.org/10.1021/ja411006a>
38. Kang SW, Yoo SP, Kim BS. Effect of chondrocyte passage number on histological aspects of tissue-engineered cartilage. *Bio-Med Mater Eng* 2007;17(5):269–76.
39. Akbari A, Li Y, Kilani RT, Ghahary A. Red blood cell lysate modulates the expression of extracellular matrix proteins in dermal fibroblasts. *Mol Cell Biochem* 2012;370(1–2):79–88. <https://doi.org/10.1007/s11010-012-1400-1>
40. Guijas C, Montenegro-Burke JR, Domingo-Almenara X, Palermo A, Warth B, Hermann G, et al. METLIN: A Technology Platform for Identifying Knowns and Unknowns. *Anal Chem* 2018;90(5):3156–64. <https://doi.org/10.1021/acs.analchem.7b04424>
41. Xia J, Sinelnikov IV, Han B, Wishart DS. MetaboAnalyst 3.0—making metabolomics more meaningful. *Nucleic Acids Res* 2015;43(W1):W251–7. <https://doi.org/10.1093/nar/gkv380>
42. Potpally N, Rodeo S, So P, Mautner K, Baria M, Malanga GA. A review of current management of knee hemarthrosis in the non-hemophilic population. *Cartilage* 2021;13(1_suppl):116S–21S. <https://doi.org/10.1177/1947603520942937>
43. Jansen NWD, Roosendaal G, Wenting M, Hazewinkel HAW, Bijlsma JWJ, Theobald M, et al. Very rapid clearance after a joint bleed knee can not prevent adverse effects on cartilage and synovial tissue: a canine *in vivo* study. *Blood* 2008;112(11).
44. Roosendaal G, Vianen ME, Wenting MJ, van Rinsum AC, van den Berg HM, Lafeber FP, et al. Iron deposits and catabolic properties of synovial tissue from patients with haemophilia. *J Bone Joint Surg Br* 1998;80(3):540–5. <https://doi.org/10.1302/0301-620x.80b3.7807>
45. Roosendaal G, Vianen ME, Marx JJM, Berg HMVD, Lafeber FPJG, Bijlsma JWJ. Blood-induced joint damage: a human *in vitro* study. *Arthritis Rheum* 1999;42(5):1025–32. [https://doi.org/10.1002/1529-0131\(199905\)42:5<1025::AID-ANR23>3.0.CO;2-3](https://doi.org/10.1002/1529-0131(199905)42:5<1025::AID-ANR23>3.0.CO;2-3)
46. Roosendaal G, Lafeber FPJG. Blood-induced joint damage in hemophilia. *Semin Thromb Hemost* 2003;29(1):037–42. <https://doi.org/10.1055/s-2003-37938>
47. Hooiveld MJJ. Haemoglobin-derived iron-dependent hydroxyl radical formation in blood-induced joint damage: an *in vitro* study. *Rheumatology* 2003;42(6):784–90. <https://doi.org/10.1093/rheumatology/keg220>
48. Narkbunnam N, Sun J, Hu G, Lin FC, Bateman TA, Mihara M, et al. IL-6 receptor antagonist as adjunctive therapy with clotting factor replacement to protect against bleeding-induced arthropathy in hemophilia. *J Thromb Haemost* 2013;11(5):881–93. <https://doi.org/10.1111/jth.12176>
49. Tiku ML, Shah R, Allison GT. Evidence linking chondrocyte lipid peroxidation to cartilage matrix protein degradation possible role in cartilage aging and the pathogenesis of osteoarthritis. *J Biol Chem* 2000;275(26):20069–76. <https://doi.org/10.1074/jbc.M907604199>
50. Rose BJ, Kooymann DL. A tale of two joints: the role of matrix metalloproteases in cartilage biology. *Dis Markers* 2016;2016, 4895050. <https://doi.org/10.1155/2016/4895050>
51. Bakker B, Eijkel GB, Heeren RMA, Karperien M, Post JN, Cillero-Pastor B. Oxygen-dependent lipid profiles of three-dimensional cultured human chondrocytes revealed by MALDI-MSI. *Anal Chem* 2017;89(17):9438–44. <https://doi.org/10.1021/acs.analchem.7b02265>
52. Rocha B, Cillero-Pastor B, Eijkel G, Bruinen AL, Ruiz-Romero C, Heeren RMA, et al. Characterization of lipidic markers of chondrogenic differentiation using mass spectrometry imaging. *Proteomics* 2015;15(4):702–13. <https://doi.org/10.1002/pmic.201400260>
53. Villalvilla A, Gómez R, Largo R, Herrero-Beaumont G. Lipid transport and metabolism in healthy and osteoarthritic cartilage. *IJMS* 2013;14(10):20793–808. <https://doi.org/10.3390/ijms141020793>
54. Beam J, Botta A, Ye J, Soliman H, Matier BJ, Forrest M, et al. Excess linoleic acid increases collagen I/III ratio and “stiffens” the heart muscle following high fat diets. *J Biol Chem*

- 2015;290(38):23371–84. <https://doi.org/10.1074/jbc.M115.682195>
55. Hennebelle M, Zhang Z, Metherel AH, Kitson AP, Otoki Y, Richardson CE, et al. Linoleic acid participates in the response to ischemic brain injury through oxidized metabolites that regulate neurotransmission. *Sci Rep* 2017;7(1):4342. <https://doi.org/10.1038/s41598-017-02914-7>
56. Lee SW, Rho JH, Lee SY, Chung WT, Oh YJ, Kim JH, et al. Dietary fat-associated osteoarthritic chondrocytes gain resistance to lipotoxicity through PKCK2/STAMP2/FSP27. *Bone Res* 2018;6:20. <https://doi.org/10.1038/s41413-018-0020-0>
57. Hooiveld M, Roosendaal G, Vianen M, Berg M van den, Bijlsma J, Lafeber F. Blood-induced joint damage: longterm effects in vitro and in vivo. *J Rheumatol* 2003;30(2):339–44.
58. Roosendaal G, TeKoppele JM, Vianen ME, van den Berg HM, Lafeber FP, Bijlsma JW. Blood-induced joint damage: a canine in vivo study. *Arthritis Rheum* 1999;42(5):1033–9. [https://doi.org/10.1002/1529-0131\(199905\)42:5<1033::AID-ANR24>3.0.CO;2-#](https://doi.org/10.1002/1529-0131(199905)42:5<1033::AID-ANR24>3.0.CO;2-#)
59. Lee AJ, Mahoney C, Cai C, Ichinose R, Stefani RM, Marra K, et al. Sustained delivery of SB-431542, a type I TGF- β 1 receptor inhibitor, to prevent arthrofibrosis. *Tissue Eng Part A* 2021;27(21–22):1411–21. <https://doi.org/10.1089/ten.TEA.2021.0029>
60. Stefani RM, Lee AJ, Tan AR, Halder SS, Hu Y, Guo XE, et al. Sustained low-dose dexamethasone delivery via a PLGA microsphere-embedded agarose implant for enhanced osteochondral repair. *Acta Biomater* 2020;102:326–40. <https://doi.org/10.1016/j.actbio.2019.11.052>
61. Roach BL, Kelmendi-Doko A, Balutis EC, Marra KG, Ateshian GA, Hung CT. Dexamethasone release from within engineered cartilage as a chondroprotective strategy against interleukin-1 α . *Tissue Eng Part A* 2016;22(7–8):621–32. <https://doi.org/10.1089/ten.TEA.2016.0018>
62. Ma L, Zheng X, Lin R, Sun AR, Song J, Ye Z, et al. Knee osteoarthritis therapy: recent advances in intra-articular drug delivery systems. *Drug Des Devel Ther* 2022;16:1311–47. <https://doi.org/10.2147/DDDT.S357386>